CRISPR-Cas9-Mutated Pregnane X Receptor (*pxr*) Retains Pregnenolone-induced Expression of *cyp3a65* in Zebrafish (*Danio rerio*) Larvae

Matthew C. Salanga [ORCID] ,*,†,1 Nadja R. Brun,† Rene D. Francolini,†
John J. Stegeman,† and Jared V. Goldstone†,1

*Department of Biological Sciences, Northern Arizona University, Flagstaff, Arizona, 86011; and †Biology Department, Woods Hole Oceanographic Institution, Woods Hole, Massachusetts, 02543

Gene/Protein Nomenclature

Gene and protein symbols follow their appropriate species-specific nomenclature guidelines. That is, for zebrafish symbols, gene and protein symbols are written in with lowercase italics or first letter capitalized regular font, respectively. For human symbols, gene and protein symbols are written in all uppercase italics or uppercase regular font, respectively. For rodent symbols, gene and protein symbols are written with first letter capitalized and italics or all uppercase regular font, respectively. When referring to genes or proteins across different species the human nomenclature guidelines are followed.

[1]To whom correspondence should be addressed at Matthew Salanga Department of Biological Sciences Northern Arizona University PO Box 5640 Flagstaff, Arizona, 86011. Tel: 928-523-5629; Fax: 928-523-7500. E-mail: matthew.salanga@nau.edu; Jared Goldstone, Biology Department Woods Hole Oceanographic Institution 266 Woods Hole Road Woods Hole, Massachusetts, 02543. Tel: 508-289-4823; Fax: 508-457-2134. E-mail: jgoldstone@whoi.edu.

ABSTRACT

Pregnane X receptor (PXR; *NR1I2*) is a nuclear receptor that regulates transcriptional responses to drug or xenobiotic exposure, including induction of *CYP3A* transcription, in many vertebrate species. PXR is activated by a wide range of ligands that differ across species, making functional studies on its role in the chemical defensome most relevant when approached in a species-specific manner. Knockout studies in mammals have shown a requirement for PXR in ligand-dependent activation of *CYP3A* expression or reporter gene activity. Morpholino knockdown of Pxr in zebrafish indicated a similar requirement. Here, we report on the generation of 2 zebrafish lines each carrying a heritable deletion in the *pxr* coding region, predicted to result in loss of a functional gene product. To our surprise, larvae homozygous for either of the *pxr* mutant alleles retain their ability to induce *cyp3a65* mRNA expression following exposure to the established zebrafish Pxr ligand, pregnenolone. Thus, zebrafish carrying *pxr* alleles with deletions in either the DNA binding or the ligand-binding domains did not yield a loss-of-function phenotype, suggesting that a compensatory mechanism is responsible for *cyp3a65* induction. Alternative possibilities are that Pxr is not required for the induction of selected genes, or that truncated yet functional mutant Pxr is sufficient for the downstream transcriptional effects. It is crucial that we develop a better understanding for the role of Pxr in this important biomedical test species. This study highlights the potential for compensatory mechanisms to avoid deleterious effects arising from gene mutations.

Key words: NR1I2; *cyp3a65*; pregnenolone; CRISPR-Cas9; zinc finger; xenobiotic.

Pregnane X receptor (PXR), also known as nuclear receptor subfamily 1, group I, member 2 (NR1I2; ZDB-GENE-030903-3), is a ligand-activated zinc finger (ZF) transcription factor that in mammals regulates transcriptional responses to drug and xenobiotic exposure, including induction of the quintessential xenobiotic-metabolizing enzyme cytochrome P450 3A (CYP3A) (Blumberg *et al.*, 1998; Kliewer *et al.*, 2002; Lehmann *et al.*, 1998; Zhou *et al.*, 2009). As with other NR1s, Pxr can roughly be divided into several functional domains consisting of an amino-terminal activation function domain (AF1), a DNA-binding domain (DBD), a

ligand-binding domain (LBD), and a carboxy-terminal AF2. Pregnane X receptor is a promiscuous nuclear receptor, activated by diverse compounds including pharmaceuticals, pollutants, and endogenous compounds (Krasowski *et al.*, 2005; Lille-Langøy *et al.*, 2015; Moore *et al.*, 2002). PXR has been identified in most vertebrates including mammals, birds, and zebrafish, and its role as a xenobiotic sensor appears conserved, although there are substantial interspecies differences in ligand specificity (Ekins *et al.*, 2008; Kliewer *et al.*, 1998; Lehmann *et al.*, 1998; Moore *et al.*, 2002). Challenging the idea of conserved function are reports that some fish (Eide *et al.*, 2018), some obligatory carnivores, and perhaps elasmobranchs have lost PXR during their evolution (Fonseca *et al.*, 2019; Hecker *et al.*, 2019). Our study begins to experimentally address the questions regarding the necessity of and roles for PXR in gene induction.

Studies in humans suggest that over half of all therapeutic drugs activate PXR, inducing expression of phases 1 and 2 biotransformation enzymes such as CYP3A, making PXR a critical regulator of drug metabolism (Lehmann *et al.*, 1998). Studies in human and rodent models, and more recently in fish, show that PXR agonists are broadly distributed in the environment from sources such as sewage effluent and industrial waste (Delfosse *et al.*, 2015; Gräns *et al.*, 2015; Kubota *et al.*, 2015). These studies suggest that PXR is in the first line of the vertebrate chemical defensome (Dussault and Forman, 2002; Goldstone *et al.*, 2006) in most vertebrates.

Although there appears to be a conserved role for PXR as a drug and xenobiotic "gate keeper," ligand specificity across species is inconsistent and requires direct testing of possible ligands to identify species-specific agonists. Notably, PXR exhibits differences in ligand-mediated activation even among mammals. For example, the human PXR agonist rifampicin does not activate rat PXR, while pregnane-16α-carbonitrile, a known rat PXR agonist, fails to activate human PXR (Igarashi *et al.*, 2012; Tirona *et al.*, 2004; Xie *et al.*, 2000). However, the steroid pregnenolone (PN) is a broadly conserved ligand across vertebrates (Kliewer *et al.*, 1998), including zebrafish (Kubota *et al.*, 2015).

Directed loss-of-function studies can establish the roles for a given gene and its product such as *PXR*. Studies using a morpholino oligonucleotide to transiently block *pxr* translation in zebrafish resulted in the loss of ligand-activated transcription of the Pxr target genes *cyp3a65* and *pxr* itself (an apparent autoinduction loop) (Kubota *et al.*, 2015). In mammals, loss-of-function has been reported in *Pxr* genetic knockouts, in which PXR ligands do not activate *Cyp3a4* transcription (Xie *et al.*, 2000). In addition, physiological abnormalities in *Pxr*-deficient rodents have been reported, including poor breeding success (Frye *et al.*, 2014), reduced bone density, premature wearing of cartilage (Azuma *et al.*, 2010, 2015; Konno *et al.*, 2010), and disrupted glucose homeostasis (Spruiell *et al.*, 2015). Studies examining natural human variants of PXR identified a single amino acid substitution (R98C) in the second ZF domain that eliminates PXR DNA binding and transactivation of *CYP3A4* in the presence of authentic PXR-ligands (Koyano *et al.*, 2004). Similarly, zebrafish allelic variants cloned and overexpressed in COS cells revealed differences in *cyp3a* luciferase reporter expression in response to clotrimazole (Lille-Langøy *et al.*, 2019).

To investigate the possibility that total loss of *pxr* in zebrafish would present transcriptional consequences consistent with those reported in the mammalian literature, and to determine further ligand-specific effects, we generated 2 genetic *pxr* mutant lines in zebrafish, using CRISPR-Cas9 RNA-guided nuclease (RGN), and tested responses of those lines to a PXR agonist. *Prima facie* interpretation of the mutations would suggest loss-of-function, but the mutant animals show activation of Pxr target transcription when exposed to pregnenolone. These results suggest either a compensatory mechanism is responsible for target gene transcription, or that a functional Pxr protein is still being translated despite the presence of mutations.

MATERIALS AND METHODS

Animal husbandry. Experimental and husbandry procedures using zebrafish were approved by the Woods Hole Oceanographic Institution's Animal Care and Use Committee. AB strain wild-type zebrafish were used in these studies. Embryos were obtained through pairwise or group breeding of adults using standard methods, rinsed with system water and moved to clean polystyrene petri dishes with 0.3× Danieau's solution (Westerfield, 2000). Embryos were cultured at 28.5°C with a 14-h light-10-h dark diurnal cycle. At 24-h postfertilization (hpf) 0.3× Danieau's solution was replaced, and all dead or defective embryos were removed. Larvae were fed daily with a diet according to their age starting with rotifers (*Brachionus rotundiformis*) at 5 dpf, then rotifers plus brine shrimp (*Artemia franciscana*) at 9 dpf. At 21 dpf, diets were supplemented with pellet feed (Gemma Micro 300, Skretting), and fish are fed brine shrimp and pellets only after 30 dpf. To anesthetize adult fish for fin biopsies, fish were immersed in fresh Tricaine (0.016% w/v; 3-amino benzoic acid ethyl ester; Sigma A-5040) in system water buffered with $NaHCO_3$ to pH 7.5 until motionless, usually 1–2 min. The tip of the caudal fin was dissected using a scalpel or razor blade and processed for genomic DNA (gDNA) extraction. Following fin biopsy, adults were returned to their aquatic habitat with normal feeding regimens in place. All biopsied fish were given at least 7 days to recover before any additional handling.

Microinjection equipment. Embryos were injected using a pneumatic microinjector (Model PV-820, World Precision Instruments). Injection needles were pulled from borosilicate capillary tubes (TW100F-4, WPI) using a vertical pipette puller (Model P-30, Sutter Instruments, Inc).

Microinjection solutions. Injection solution (1–2 nl) was targeted to the 1-cell embryo at the interface between the embryo and underlying yolk. Injection solutions consisted of combinations of 1 μg/μl Cas9 recombinant protein (PNA Bio, CP-01) or 400 ng/μl Cas9 mRNA (Addgene plasmid No. 51307; Guo *et al.*, 2014), and 200 ng/μl H2B-RFP mRNA (Myers and Krieg, 2013) and pooled single guide RNA (sgRNAs) at 100–200 ng/μl for each sgRNA (Supplementary Table 1).

Polymerase chain reaction. Endpoint PCR for genotyping or sgRNA template preparation was carried out using Q5 (M0491 NEB) or *Taq* (M0267 NEB) polymerase and corresponding reaction buffers. Genotype PCR assembly included template (20–200 ng gDNA or cDNA), dNTPs at 200 μM final, forward and reverse primers at final concentration 300 nM (for *Taq* reaction) or 500 nM (for Q5 reaction), and polymerase-specific reaction buffer at 1× final concentration, and Q5 at 0.02 U/μl or *Taq* at 0.025 U/μl, reaction volumes range from 20 to 100 μl, and component input were scaled according to reaction size. For sgRNA template preparation proceeded essentially as described in Bassett *et al.* (2013), Gagnon *et al.* (2014), and Nakayama *et al.* (2014). Briefly, universal reverse primer was combined with a forward primer containing a 5′ T7 polymerase binding site, gene-specific target
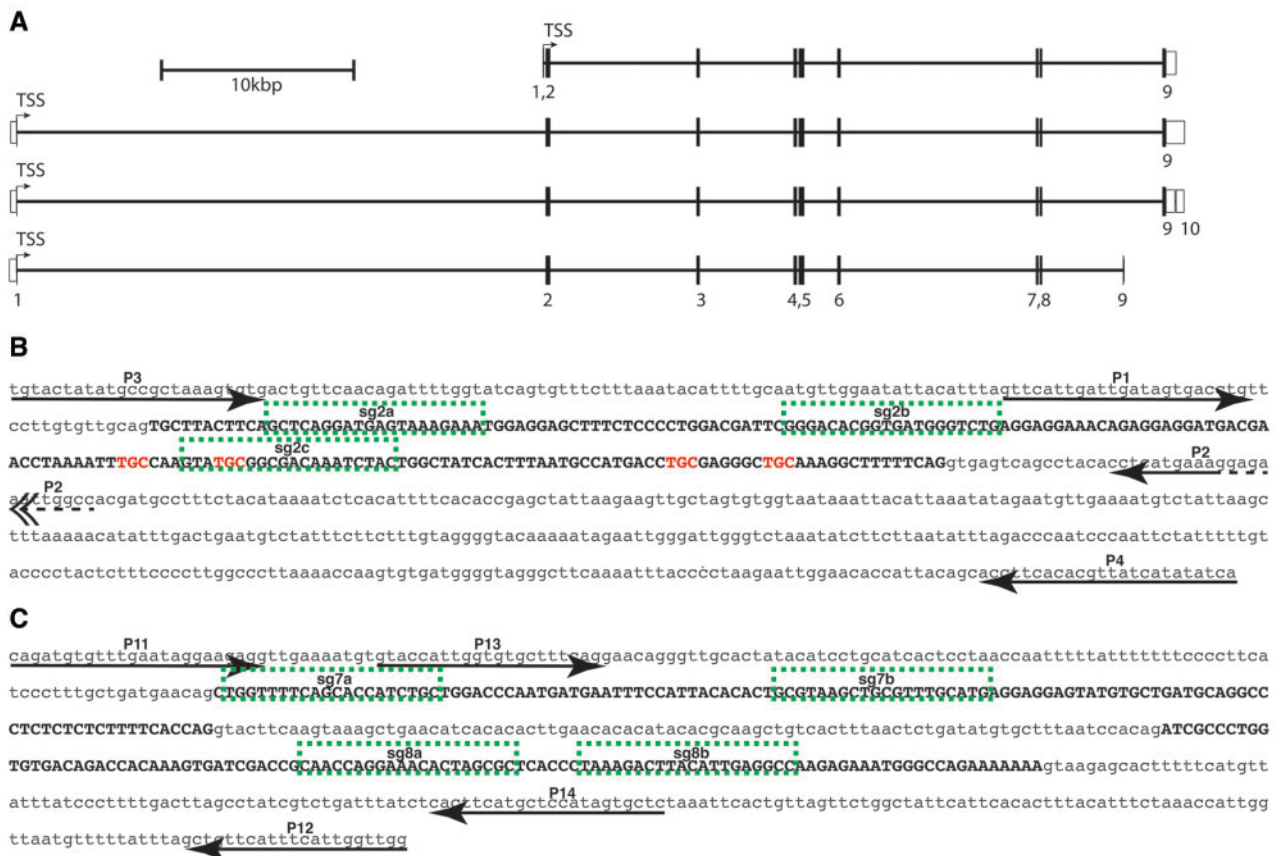
Figure 1. Zebrafish *pxr* gene models, single guide RNA target sites and PCR primer locations. A, Merged ENSEMBL/Havana gene models identify 4 transcript variants (ZDB-GENE-030903-3; Chromosome 9:9 524 490–9 584 607). Numbered exons are shown as open bars for untranslated sequence or solid bars for coding regions. Translational start sites reside in exon 1 for all transcripts. Intronic regions are shown as horizontal black line spanning exons. B, Sequence of exon 2 (black uppercase text) and adjacent intronic regions (gray lowercase text) are shown. Position and orientation of PCR primers are shown for primers P1–P4 (arrows; also see Supplementary Table 2). Single guide RNA target sites are labeled, sg2a, sg2b, sg2c, and outlined (green or gray hashed boxes). Trinucleotides coding for zinc finger cysteine residues are shown in red or gray lettering. C, Sequence of exons 7 and 8 (black uppercase text) and adjacent intronic regions (gray lowercase text) are shown. Position and orientation of PCR primers are shown for primers P11–P14 (arrows; also see Supplementary Table 2). Single guide RNA target sites are labeled, sg7a, sg7b, sg8a, sg8b, and outlined (green or gray hashed boxes).

sequence and approximately 20 nucleotides of 3′ complementary sequence to the universal reverse primer were combined in a 100 µl reaction at 500 nM final concentration for each, dNTPs at 200 µM final, Q5 reaction buffer at 1× final concentration, and 2 U of Q5 (Supplementary Table 1). PCR products were visualized by agarose gel electrophoresis and nucleic acid staining with SYBR safe DNA stain (S33102, Thermo Fisher Scientific), and imaged with an EZ Gel Documentation System (Bio-Rad, 1708270 and 1708273). Purification of PCR products was done using PCR QIAquick PCR cleanup kit (Qiagen, 28106), according to product instructions. Primer sequences and cycling conditions are reported in (Supplementary Table 2).

Single guide RNA site selection and synthesis. Coding sequence of *pxr* exon 2 (ZFIN: ZDB-GENE-030903-3) was queried for putative targets using the web tool "CHOPCHOP" (Howe *et al.*, 2013; Montague *et al.*, 2014) and the zebrafish GRCv10 genome. From this, we selected 3 targets opting for sequences that contained a G nucleotide within the first 3 nucleotides of the target sequence and zero predicted off-target sites. Single guide RNA sequences were additionally checked by BLAST searches. By using 3 different sgRNA targeted to the same region we should have minimized off-target effects, and subsequent outcrossing of the identified F0 lines we should additionally have decreased

nonlinked off-target mutations. Multiple nonoverlapping targets, "sgEx2-a, -b, -c; sgEx7-a, -b; sgEx8-a, -b" were selected that met the aforementioned criteria (Figure 1B; Supplementary Table 1). Briefly, DNA consisting of 80–200 ng purified PCR product (see *Polymerase chain reaction—sgRNA template preparation*) was used in MEGAscript (Ambion, AM1330) or MAXIscript (Ambion, AM1309) *in vitro* transcription reactions according to product instructions with 37°C incubation lasting between 4 and 5 h and 80 ng template DNA for MAXIscript, and 200 ng template DNA for MEGAscript reactions.

RNA isolation. Total RNA was isolated from embryonic or larval tissue by mechanically homogenizing the tissue at room temperature in 500 µl TRIzol (Ambion, 15596-018) followed by RNA isolation according to TRIzol product instructions, or using a Direct-zol RNA MiniPrep Plus kit (ZYMO Research Corp, 2072). Contaminating gDNA was removed from the TRIzol isolated RNA by enzymatic digestion with 10U of Turbo DNase (Ambion, AM2239) at 37°C for 15 min, in a reaction tube for TRIzol-mediated extractions or on ZYMO RNA MiniPrep spin columns. DNase was removed from the RNA by organic extraction with phenol:CHCl3:IAA (isoamyl alcohol) (125:24:1) and followed with CHCl3:IAA (24:1), precipitated by adding 10%v/v 3 M pH 5.2 sodium acetate solution and 2.5 volumes of 100% ice-cold ethanol

and cooled to -20°C for ≥ 20 min then centrifuged at 16–20 kRCF for 20 min. The RNA pellet was washed 2 times with 70% EtOH, air dried and dissolved in 20–50 μl DNase/RNase-Free water. RNA isolated using ZYMO Direct-zol RNA MiniPrep column was eluted in 50 μl DNase/RNase-Free water. Final concentration was measured by 260/280 nm absorbance on a Nanodrop 2000. The integrity of total RNA was confirmed on a minority of samples by agarose gel electrophoresis and visual inspection of 28 s and 18 s ribosomal RNA bands.

cDNA synthesis for real-time PCR quantitation. DNA-free RNA was reverse transcribed using iScript cDNA Synthesis Kits (Bio-Rad, 170-8891) according to product instructions. RNA template amount was standardized across treatments for each experiment ranging from 400 ng for individual embryos to 1 μg for pooled samples. RNA was primed with a mix of random hexamers and oligo-dT included with the kit.

cDNA synthesis for cloning. Up to 1 μg of DNA-free RNA was reverse transcribed using ProtoScript II Reverse Transcriptase (NEB, M0368), and anchored oligo-dT primers according to product instructions.

Real-time PCR. Quantitative real-time PCR was conducted on a CFX96/C1000 Real-time detector and thermocycler (Bio-Rad). iQ SYBR Green Supermix (Bio-Rad, 170-8882) or SsoFast EvaGreen Supermix (Bio-Rad, 172-5203) was used for reaction assembly as per product instructions. Real-time runs incorporated experimental templates, no template controls, and minus-RT controls, conducted with technical duplicates. $\Delta\Delta$Ct relative quantification was performed using Bio-Rad CFX Manager software (CFX Manager Version 3.1; Hercules, California) normalized to zebrafish housekeeping genes, *ef1a* and *arnt2*. Cycling conditions were 95°C—3 min; [95°C 10 s, 60°C 30 s]*40 cycles for iQ SYBR and 95°C—30 s; [95°C 5 s, 60°C 5 s]*40 cycles for SsoFast EvaGreen. Fluorescence was recorded during annealing-extension (ie, 60°C). Melt curve analysis was performed over 65°C–95°C temperature range in 0.5°C increments and 5 s per dwell time per step. See Supplementary Table 3 for quantitative PCR primer sequences.

Genomic extraction. Genomic DNA was isolated from adult fin biopsies or individual or pooled embryos 24–72 hpf. Briefly, embryos still in their chorion or single fin biopsies from anesthetized adult fish were collected and homogenized in 200 μl 10 mM Tris-HCl, 100 mM EDTA, 0.5% w/v SDS, 200 μg/ml proteinase K at 56°C for > 1 h or overnight. Homogenates were organically extracted with phenol:CHCl$_3$:IAA (49.5:49.5:1) and followed with CHCl$_3$:IAA (24:1). Extracts were precipitated by adding 10%v/v 3 M pH 5.2 sodium acetate solution and 2.5 volumes of 100% ice-cold ethanol and cooled to -20°C for ≥ 20 min. To pellet the gDNA, precipitation solutions were centrifuged at 4°C and 16–20 kRCF for 20 min. gDNA pellets were washed twice with an equal volume of 70% EtOH, air dried at room temperature and dissolved in 10–20 μl of nuclease-free deionized H$_2$O per individual embryo (eg, gDNA from pool of 5 embryos dissolved in 50–100 μl). Final gDNA concentration was measured by 260/280 nm absorbance on a Nanodrop 2000 spectrophotometer (Thermo Fisher Scientific).

mRNA synthesis. CS2-plasmid (1–5 μg) containing the open reading frame (ORF) for Cas9 (Addgene No. 51307) or H2B-RFP was linearized by Not1 endonuclease digestion, followed by phenol:CHCl$_3$:IAA extraction and EtOH precipitation. One microgram linearized plasmid was used as template in SP6 mMessage mMachine *in vitro* transcription reaction (Ambion, AM1344) according to product instructions.

Chemical exposure. The zebrafish Pxr agonist, pregnenolone (5-pregnen-3β-ol-20-one, PN, CAS No. 145-13-1), was dissolved in 100% DMSO at a concentration of 100 mM, and diluted in 0.3× Danieau's solution for a final concentration of 3 μM PN/0.05% v/v DMSO. Forty-eight hpf embryos were exposed as individuals or groups for 24 h to 0.05% v/v DMSO (vehicle control) or 3 μM PN/0.05% v/v DMSO, in multiwell, plates at a volume of 1 ml solution per included individual (eg, 5 individuals in 5 ml treatment solution). Following exposure embryos (groups or individuals; whole or dissected) were snap-frozen in liquid N$_2$ and stored at -70°C until processing. Exposure experiments were all performed at least twice.

Statistics. One-way ANOVA and Tukey's multiple comparison tests were performed for gene expression data using Prism GraphPad Version 6 (GraphPad Software, San Diego, California). Significance levels were set at $\alpha < .05$.

RESULTS

The zebrafish *pxr* locus spans approximately 65 kb on chromosome 9 and contains 9 or 10 exons with coding sequence contained in exons 1–9 (Figure 1A). Two different *pxr* lines were generated, each carrying a large deletion in the *pxr* locus. One zebrafish line harbors a 108-bp deletion in exon 2 that includes coding sequence for the DBD and results in a frame shift and subsequent early termination codon that is detectable in the expressed transcripts. The second line is characterized by a 236-bp deletion, including a 37-bp deletion in exon 7 and total deletion of intron 7 and exon 8. The expressed transcript from the exon 7, 8 mutant allele revealed direct splicing of exons 6–9.

Exon 2 Targeting
Four *pxr* splice variants have been identified in zebrafish, with exon 1 contributing to a short sequence of amino acids for all transcript variants (Figure 1A) (Yates *et al.*, 2016). The sequence of exon 2 is entirely coding and conserved among the 4 identified transcript variants, and therefore was selected as the primary locus for RGN targeting (Figure 1B). Pxr contains 2 C4 ZFs in its DBD, and exon 2 encodes all 4 cysteine residues in the first ZF, thought to be necessary for C4 ZF structures in general (Figure 1B). Thus, it seemed reasonable to predict a lesion in the ZF domain would compromise the ability for Pxr to bind *cis*-regulatory units and therefore abrogate its capacity for transactivation of target genes such as *cyp3a65*. Three nonoverlapping (sgRNAs targets in exon 2 were identified and sgRNA was synthesized (Supplementary Table 1).

Exons 7 and 8 Targeting
Exons 7 and 8 of the *pxr* locus are coding, contribute to the LBD, and are contained in all known splice variants (Figure 1A). Four nonoverlapping sgRNA target sites, 2 in exon 7 and 2 in exon 8 were identified and sgRNAs were synthesized (Figure 1C, Supplementary Table 1).

Confirmation of Mutagenesis
Genomic extracts from pooled RGN-injected or uninjected sibling control embryos (5–10 embryos per pool; 24–48 hpf) were isolated and probed by PCR using primers flanking the RGN
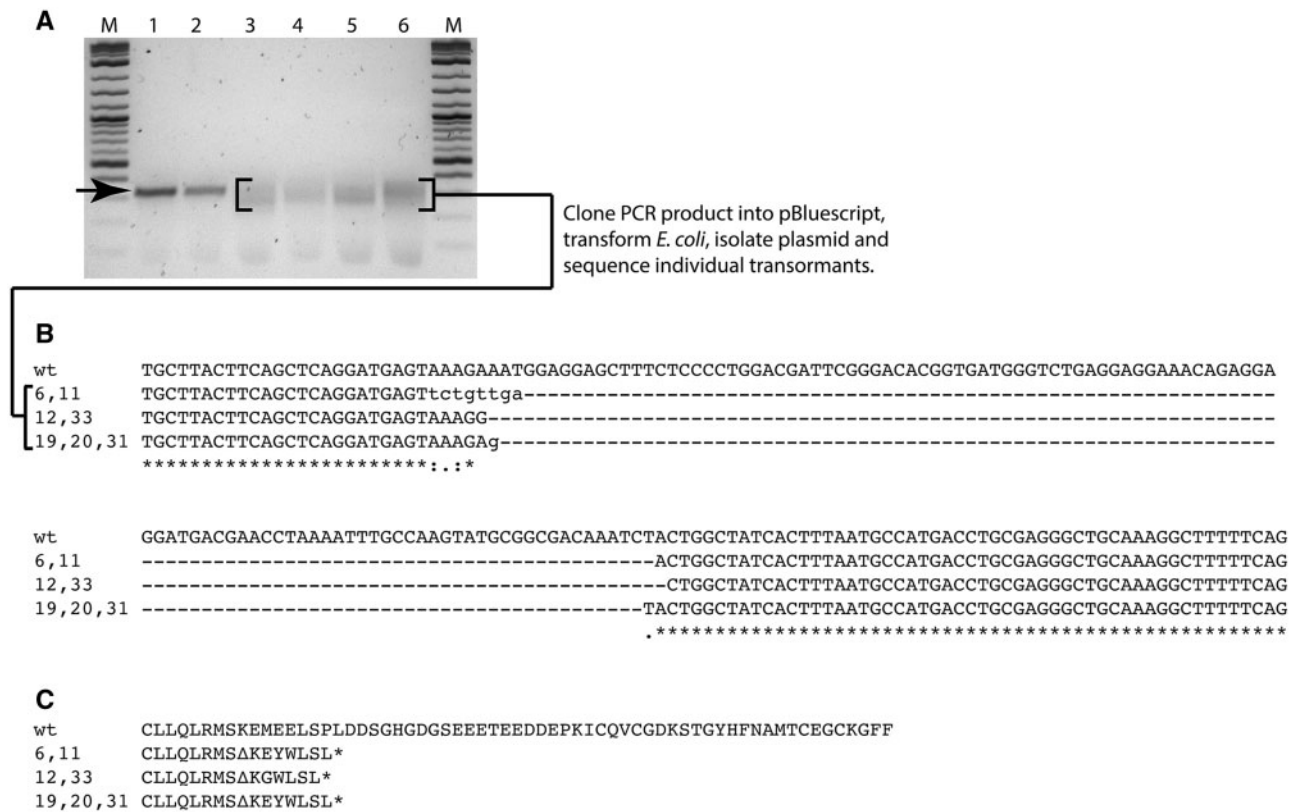
Figure 2. *pxr* genotyping of F0 embryos. A, Gel image showing PCR products derived from 24 hpf RNA-guided nuclease (RGN)-injected F0 founder (lanes 3–6) or uninjected control (lanes 1 and 2) embryos primed using primers P1 and P2 as shown in Figure 1B). Single band migrating at approximately 350 bp is apparent for control embryos (arrow, lanes 1 and 2). A smear migrating from approximately 350–200 bp is visible for RGN-injected embryos (bracket, lanes 3–6). 2-Log DNA ladder (lanes M, NEB). B, Sequences for deletion-mutant exon 2 locus from 7 F1 $pxr^{e2/+}$ are aligned to wt. Three mutant alleles are observed. C, Hypothetical translation of exon 2 for pxr^{e2} alleles. Mutant alleles contain deletions (—), missense mutations (lower case text), and early translation termination codons (asterisk).

target sites (Figs. 1B and 1C). PCR products derived from uninjected control embryos migrated as a single band at the predicted wildtype length, whereas PCR products from exon 2 RGN-targeted embryos migrated as a molecular weight smear and a near absence of a wildtype-sized band, as shown for exon 2 targets in Figure 2A, or as a wildtype-sized band and reduced size band as observed in exons 7-, 8-targeted mutants (data not shown). F0 CRISPR mutants (ie, founders) will almost always contain mosaic patterns of gene-edited alleles. We therefore would expect a variety of amplicon lengths that are likely to form heteroduplexes during reannealing and elongation phases of PCR, adding amplicon length diversity to the reaction product, appearing as a smear or multiple bands. PCR amplicons from control and injected embryos were subsequently cloned into pBluescript vector (Stratagene) and Sanger sequenced to obtain sequence-specific allele information. This revealed a range of deletion alleles some containing missense mutations, including a 108-bp deletion in the pxr^{e2} cohort (Figure 2C) and 236-bp deletion in the pxr^{e7e8} cohort (Supplementary Figure 1) compared with wildtype control amplicons. The remaining RGN-injected embryos were raised to sexual maturity as putative F0 founders.

Phenotypically, the pxr^{e2} and pxr^{e7e8} CRISPR mutants have no obvious impairments. Mutant larvae developed into adults that had no evident swimming or feeding issues, and that are morphologically indistinguishable from wildtype adults. Sexually mature mutants spawned readily to produce embryos and larvae, which had no obvious impairments. However, there was a trend toward a slight (ca. 5% by 3 dpf) but consistent decrease in length in the pxr^{e7e8} CRISPR mutant larvae (Supplementary Figure 2).

Outcross and Genotyping of F1 Generation

Individual F0 putative founder adults were outcrossed with wildtype AB strain individuals to generate putative heterozygote F1 embryos. A subset of these F1 embryos was sacrificed, gDNA extracted, and PCR probed to confirm transmission of mutant alleles through visualization of reduced PCR product size (Figure 2B; Supplementary Figure 3). The remaining sibling embryos were raised for approximately 4 weeks and nonlethal fin biopsies were taken from individual fish for DNA extraction and PCR amplification of the targeted region. The PCR amplicons were purified and Sanger sequenced to identify sequence-specific genotypes (Figure 2C). A variety of genotypes for each of the targeted exons were obtained including a cohort of individuals with an approximate 108-bp deletion in exon 2. Computational translation of the mutant alleles showed the introduction of missense mutations and early termination codons (Figure 2C). A second cohort with a 236-bp deletion spanning from exon 7 to exon 8 (Supplementary Figure 1) was verified after (but not before) F1 outcrossing and revealed a single mutant allele. Mutant alleles from the pxr^{e2} and pxr^{e7e8} mutant cohorts segregated according to Mendelian principles of inheritance (data not shown).

Response to Pregnenolone in Wildtype and Mutant F2 Larva

Individual F2 embryos from pxr^{e2} F1 heterozygote crosses (prior to genotyping) were exposed to 3 μM pregnenolone (PN) or vehicle control (DMSO 0.05% v/v) from 48 to 72 hpf, followed by dissection, gDNA extraction and PCR genotyping (Figs. 3A–E and 4A). To confirm transcription of mutant alleles, RNA from a
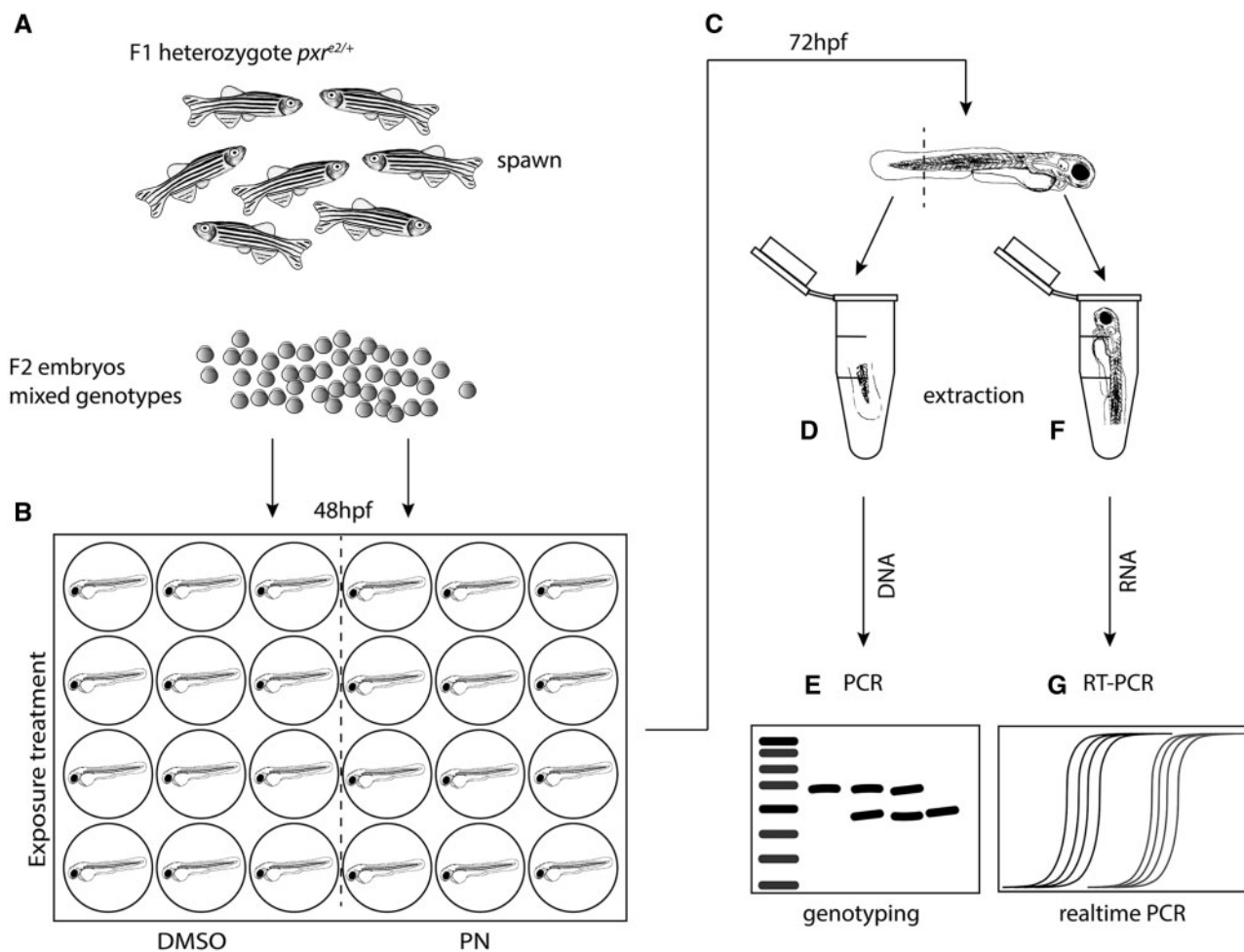
Figure 3. Schematic representation of experimental approach for individual embryo exposures to DMSO or PN and Pxr-target gene expression assessment. A, Adult F1 heterozygotes *pxr*[e2/+] were incrossed to produce mixed genotype embryos. B, At 48 hpf embryos were transferred to 24 or 48 well plates containing 0.3× Danieau's/ 0.05% v/v DMSO or 0.3× Danieau's/0.05% v/v DMSO/3 μM PN, and incubated until 72 hpf. C, Seventy-two hpf larvae were cut separating anterior (head/trunk) from posterior (tail) and moved to individual microcentrifuge tubes. D, Genomic DNA isolation was carried out on tail segment. E, PCR and gel electrophoresis were used to determine genotype. F, Total RNA was extracted from anterior portion; (G) and reverse transcribed into cDNA for quantitative real-time PCR analysis.

subset of F2 embryos was reverse transcribed into cDNA and PCR amplified with primers targeting exon 1 (forward) and exon 3 (reverse). PCR products were visualized by gel electrophoresis and showed banding patterns consistent with wildtype (wt), mutant (mut), and heterozygous (het) alleles (Supplementary Table 2; Figs. 4B and 4C). Total RNA from wt and mut embryos was extracted, reverse transcribed into cDNA and probed by quantitative real-time PCR (qPCR) for levels of the Pxr-target genes, *cyp3a*65 and *pxr* (Figs. 3F and 3G; 4C and 4D). Vehicle control-treated wt and mut larvae show similar levels of *pxr* basal transcription, suggesting similar stability for mut and wt RNA, and both showed a canonical upregulation of *cyp3a*65 and *pxr* when exposed to PN (Figure 4D). A similar experiment conducted in F3 progeny of *pxr*[e2] (Figure 5), *pxr*[e7e8] (Figure 6), or wild-type cohorts (6 pools of 5 larvae per condition) also showed a canonical response to PN exposure and revealed enrichment of *cyp3a*65 and *pxr* transcripts in PN but not vehicle exposed animals, consistent with previous experiments (Figs. 5 and 6).

Cloning **pxr** *cDNA From Mutant and Wildtype Fish*
Total RNA was extracted from mut and wt individuals and reverse transcribed into cDNA using oligo-dT priming. Primers targeting the 5′ and 3′UTRs of *pxr* mRNA were used to amplify

the full ORF (Supplementary Table 2). In addition, Sanger sequencing of *pxr*[e2] ORF and subsequent translation shows the presence of a frame shift and early termination codon at the 3′ end of exon 2, however exons 1 and 3–9 appear wildtype (Figure 7). Sequencing of *pxr*[e7e8] indicates direct splicing of exons 6–9 and absence of exons 7 and 8 in the mature transcript (Figure 7).

DISCUSSION

Zebrafish are an important model for evaluating organismal responses to toxic chemical exposure in both biomedical and ecological contexts (Stegeman *et al.*, 2010). Integrating genome editing with toxicological studies enables mechanistic investigation into the initiating events, interactions, and adverse outcomes, advancing our understanding of the role and requirements of key proteins and their molecular targets in the chemical defensome (Goldstone *et al.*, 2006). The *pxr*[e2] mutant allele lacks more than 100 nucleotides from exon 2, including nucleotides encoding 2 of the 4 cysteines in the first ZF domain, causing a frame shift mutation that generates premature termination codons. General cell and molecular biology principles instruct us that a genomic lesion which generates a frame shift in
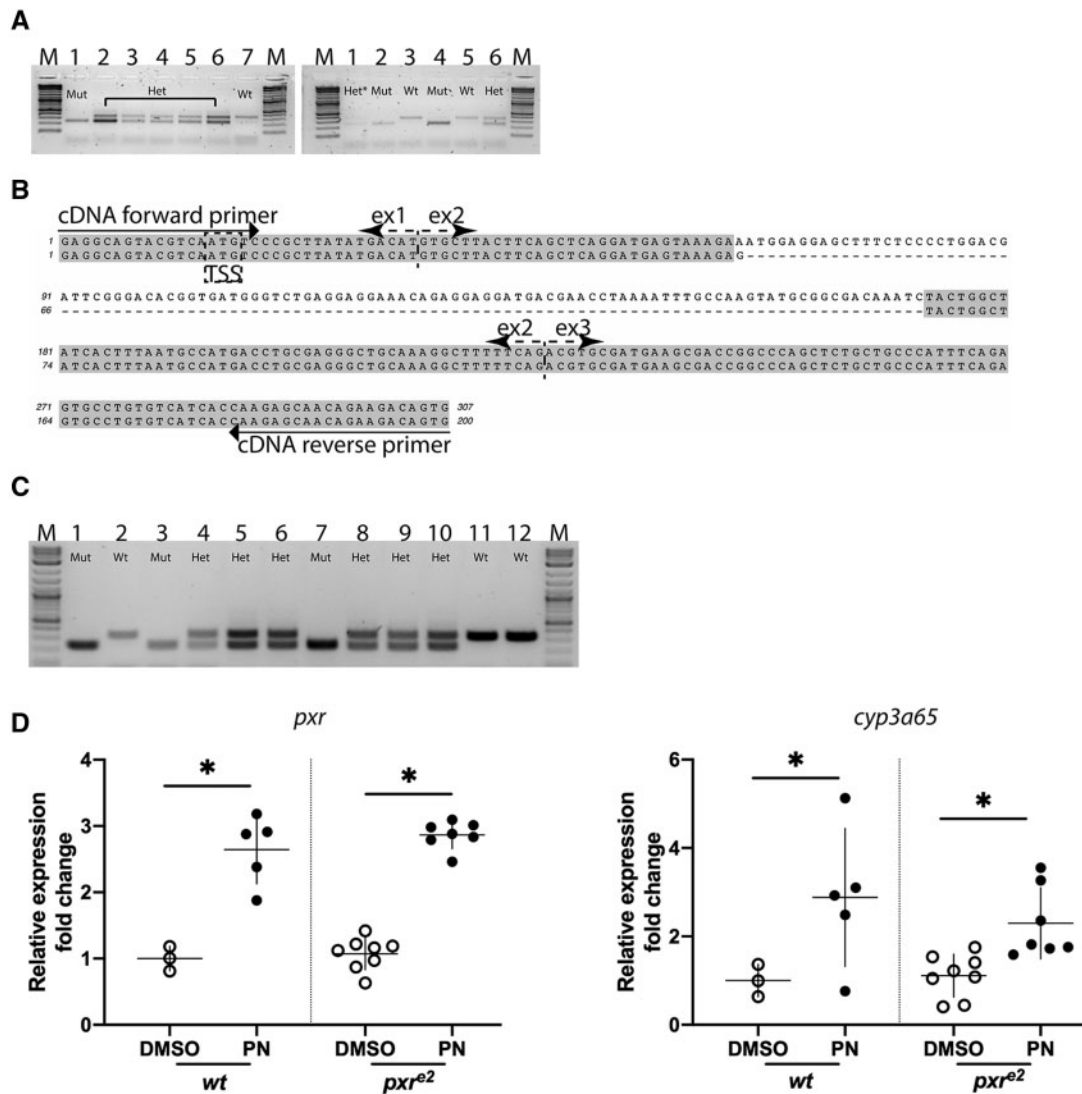
Figure 4. Post hoc exon 2 genotyping and gene expression of *pxr* and *cyp3a65* in 72 hpf wildtype and mutant embryos exposed to PN or vehicle control (DMSO). A, Gel image showing PCR products derived from genomic DNA templates using P1/P2 primers (also see Figure 2, Supplementary Table 2), show the presence of 3 product types, single lower band (Mut), upper and lower bands (Het), and single upper band (Wt). Lane marked "Het*" display weakly stained upper and lower bands. 2-Log ladder is used for size comparison (lanes M, NEB). B, Sequence spanning exons 1–3 of transcribed mutant (bottom) allele is aligned to wildtype (top) sequence. Gray highlighted text matches wildtype sequence, whereas hashed line shows deleted region. Exon (ex), translational start site. Primer location and orientation are shown (arrow). C, Gel image showing RT-PCR products from cDNA primers (also see Supplementary Table 2). Mut (lanes 1, 2, 7), Het (lanes 4–6, 8–10), and Wt (lanes 2, 11, 12) show single lower band, double band, or single higher band, respectively. D, Scatter plot showing relative expression levels for the pregnane X receptor-target genes *pxr* itself and *cyp3a65*. *pxr* and *cyp3a65* gene expression in individual larva are grouped by treatment (DMSO vs PN) and genotype (Wt vs Mut). Values are compared using 1-way ANOVA, *$p < .05$.

a coding exon should, in fact, destroy the function of the protein through missense mutations, introduction of early translational termination codons and nonsense-mediated decay. Direct deletion of 236 bp through the exons 7 and 8 region results in an alternative splice form that directly joins exons 6–9, effectively removing major components of the LBD, helices α8 and α9 and connecting loops.

The *pxr* gene resides on chromosome 9 with no evidence for a second copy or paralog (Yates et al., 2016). Four transcript variants are reported for zebrafish *pxr* containing 9 or 10 exons (Howe et al., 2013). In zebrafish there is no evidence for naturally occurring *pxr* splice variants lacking 1 or more functional domains, however in other systems, namely mammalian cell culture, alternative splicing, and sequence polymorphisms result in a variety of transcript variants, including some with

reduced function (Koyano et al., 2004; Lamba et al., 2004, 2005; Lin et al., 2009; Matic et al., 2010). Furthermore, Lille-Langøy et al. showed zebrafish *pxr* alleles containing various SNPs differentially induce reporter gene activation upon exposure to clotrimazole (Lille-Langøy et al., 2019). However, exposure to clotrimazole or the known human pxr ligand, rifampicin, did not induce endogenous *pxr* or *cyp3a65* expression, suggesting a possible disconnect between *in vitro* and *in vivo* studies (Salanga et al., unpublished data).

In this article, we report on the generation of 2 mutant zebrafish lines, each carrying a heritable deletion mutation in the *pxr* locus, with 1 affecting exon 2 (*pxr^e2*) and the other affecting exons 7 and 8 (*pxr^e7e8*). The *pxr* allele in *pxr^e2* animals lacks 108 bp in exon 2, which results in a nonsense mutation. The *pxr^e7e8* animals lack 236 bp that span from exon 7 through intron
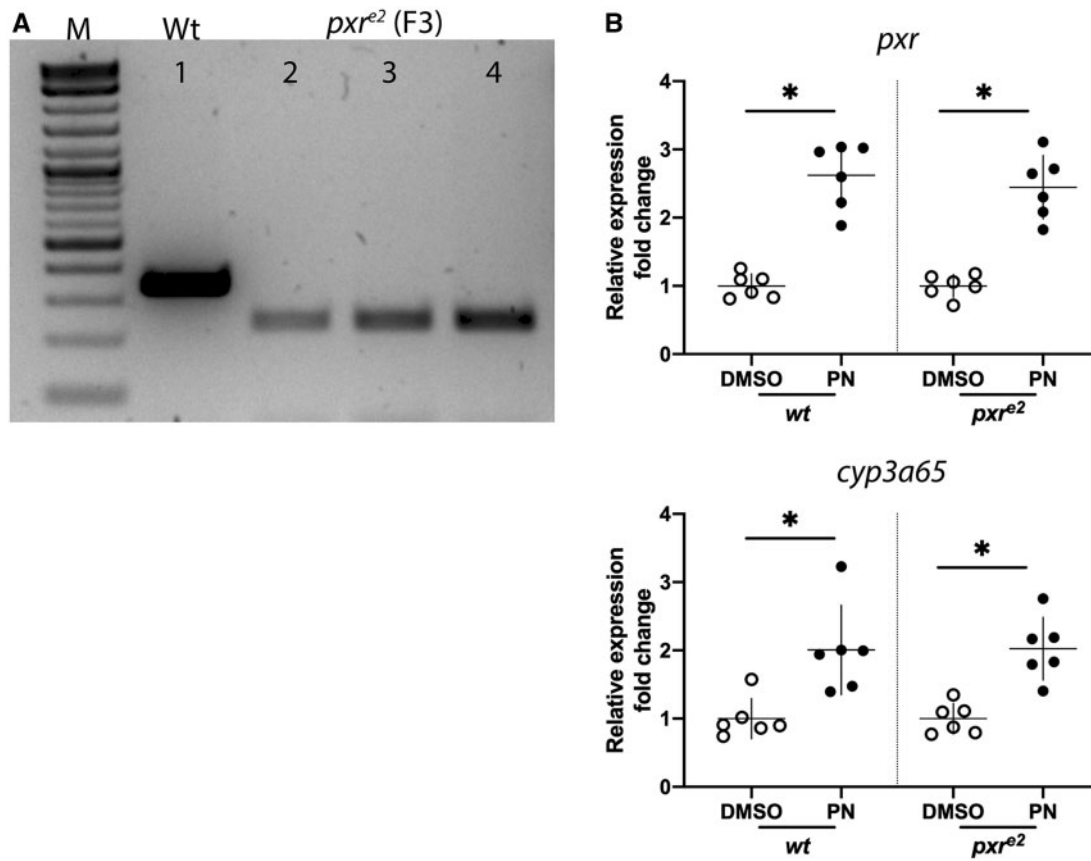
Figure 5. Genotype confirmation and target gene expression in *pxr^e2* F3 larva exposed or not exposed to PN. A, Gel image of PCR products derived from progeny of Wt (lane 1) or F2 *pxr^e2* (lanes 2–4). B, Relative expression of the Pxr-target genes, *pxr* and *cyp3a65*, derived from pooled larvae exposed to PN or vehicle control (DMSO) from 48 to 72 hpf. Each circle or dot represents 1 pool of 5 larvae. Expression levels are relative to vehicle-treated cohort of same genotype. Values are compared by 1-way ANOVA, *$p < .05$.
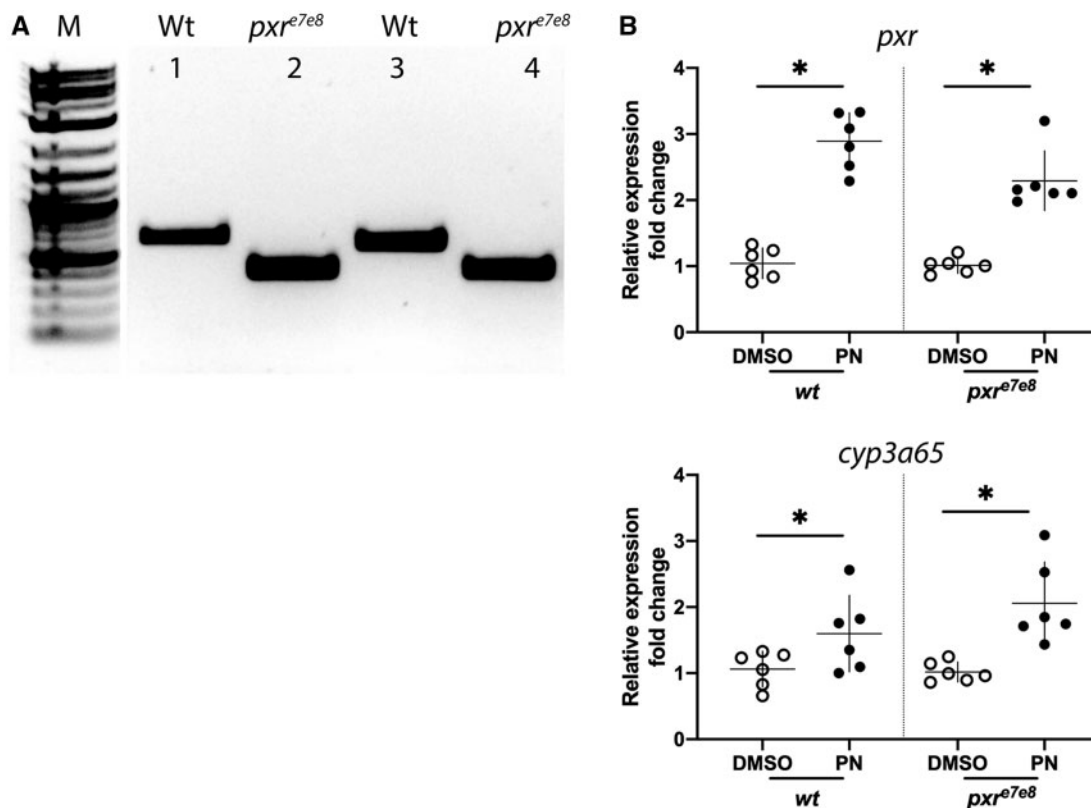
Figure 6. Genotype confirmation and target gene expression in *pxr^e7e8* F3 larva exposed or not exposed to PN. A, Gel image of PCR products derived from progeny of Wt (lanes 1 and 3) or *pxr^e7e8* (lanes 2 and 4). B, Relative expression of the Pxr-target genes, *pxr* and *cyp3a65*, derived from pooled larvae exposed to PN or vehicle control (DMSO) from 48 to 72 hpf. Each circle or dot represents 1 pool of 6 larvae. Expression levels are relative to vehicle-treated cohort of same genotype. Values are compared by 1-way ANOVA, *$p < .05$.
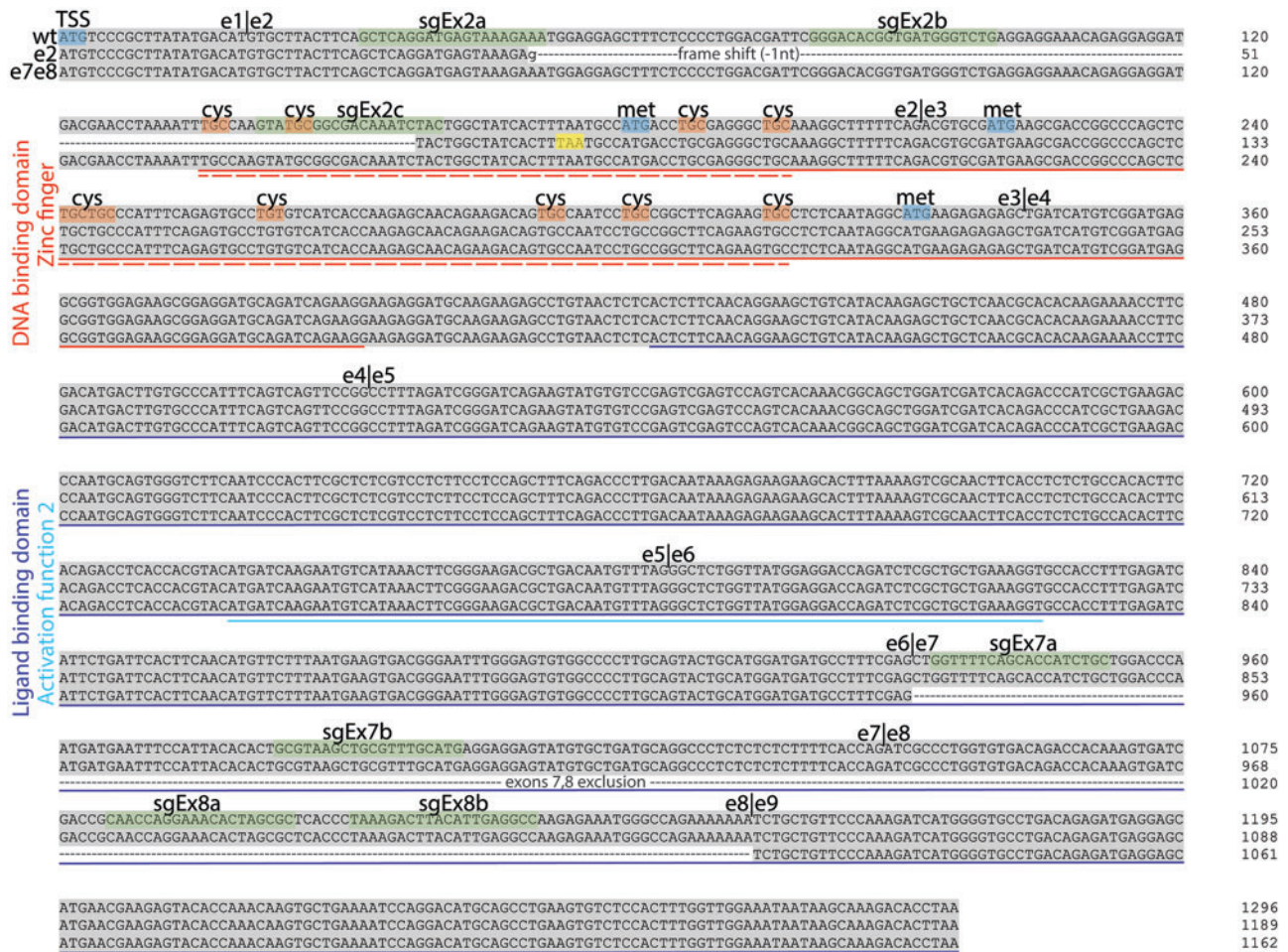
Figure 7. Domain map and sequence alignment of *pxr* wildtype, *pxr^e2^* and *pxr^e7e8^*cDNA. Single guide RNA targeting sites are highlighted in green and numbered (see also Supplementary Table 1). Red underline marks putative DNA-binding domain and red dashed underline marks zinc finger (ZF) domains. The C4 ZF cysteine codons are highlighted in orange and labeled "cys." Blue underlined sequence marks ligand-binding domain and cyan underline marks the activation function 2 domain. Exon boundaries are indicated with vertical black lines and labeled "e No." Wildtype in frame methionine codons are highlighted in blue for exons 2 and 3 and labeled with "met." The *pxr^e2^* mutant coding region shows 108-bp deletion and −1 bp frameshift and early *opal* termination codon highlighted in yellow. The *pxr^e7e8^* mutant cDNA shows a deletion of exons 7 and 8.

7 and into exon 8, resulting in a frame shift and early stop codon in the transcript. We predicted that mutations would result in premature translational termination, eliminating function. In physiological terms we expected the mutations to recapitulate the loss-of-function outcomes observed from morpholino knockdown studies in zebrafish (Kubota *et al.*, 2015) and genetic knockout studies in rodents (Xie *et al.*, 2000), essentially abrogating ligand-activated induction of target genes, such as *PXR* and *CYP3A*. Based on current zebrafish *pxr* gene models, 4 full-length transcripts have been identified containing identical exons 2–8 with variability detected in exons 1, 9, and 10. Exon 2 is the first completely coding exon for all 4 transcript models and contains the partial sequence for 1 of 2 ZF domains that comprise the DBD of the normal protein (Figure 1A). Despite the loss of 2 of 4 cysteine residues identified as components of Pxr's N-terminal most C4 ZF in the *pxr^e2^* mutant, the mutant's response to PN exposure is indistinguishable from wildtype suggesting a functional protein is being made (Figs. 4 and 5). Cloning of the full mRNA from mutant and wildtype confirms the expression of the mutant mRNA, arguing against alternative splicing as a mechanism for avoiding the mutated exon 2. An important hypothesis is that translational machinery is "ignoring" the genomic lesion transcribed into the message by using an alternative start site downstream of the genomic lesion, possibly in exon 3, thereby avoiding total loss of the protein in exchange for a truncated yet functional product (Figure 8). If we assume that translational skipping is occurring and that such translation begins at the end of exon 2 or beginning of exon 3, then the resulting protein would lack one of its ZF domains (Figure 8B). We would expect that this would inhibit the protein's ability to bind DNA, which would seem a prerequisite for transactivation. Our data suggest transactivation is occurring, and therefore we surmise that a truncated Pxr is occupying *cis*-regulatory elements on target genes. We hypothesize that this may be because PXR physically interacts with RXR in the nucleus (Ihunnah *et al.*, 2011), and thus in a zebrafish Rxr may be responsible for stabilizing Pxr binding, even in the absence of complete ZF domains.

In the *pxr^e7e8^* mutants, cloning of messenger RNA indicated a direct splicing of exons 6–9 effectively skipping the 2 targeted exons (Figs. 7 and 8), which if translated would result in a shortened protein. These observations point to the adaptability of transcription and translation in organisms and highlight how genome editing technology can illuminate these processes by
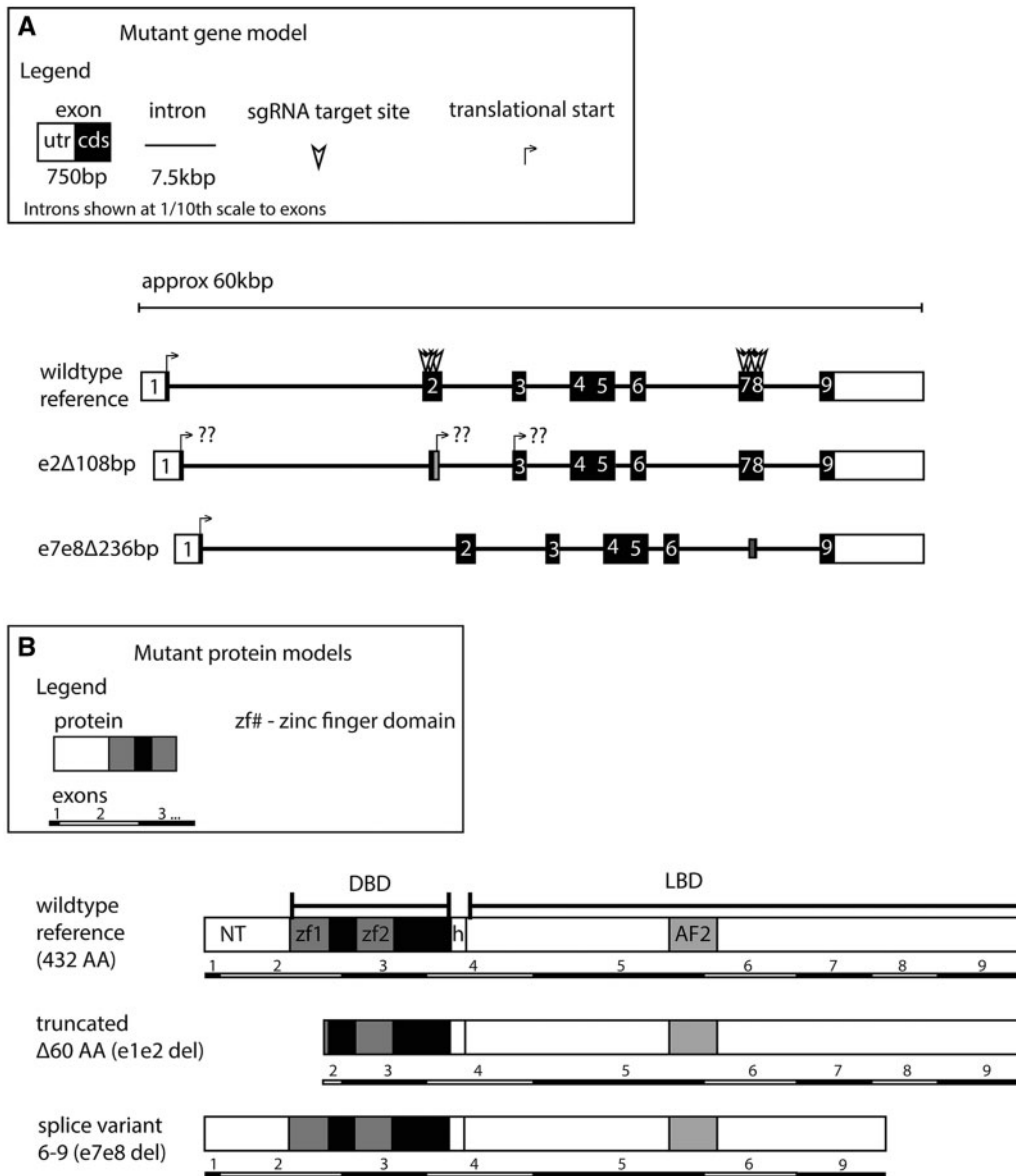
Figure 8. Models for gene structure and protein products for wildtype, *pxr*[e2] and *pxr*[e7e8] alleles. A, Line diagram showing hypothetical gene model for *pxr*[e2] and *pxr*[e7e8] compared with wildtype. *pxr*[e2] model (middle) shows a shorter exon 2 and region of frame-shifted bases downstream of the lesion. Locations of potential alternative translational start site according to wildtype frame and 3′ of the mutated region in exons 2 and 3 are marked (bent arrow and "??"). The *pxr*[e7e8] gene model (bottom) shows a partial deletion of exons 7 and 8 and total removal of intron 7. B, Hypothetical protein products supposing canonical TSS of wildtype (top) and Pxr[e7e8] (bottom) or alternative in frame translational initiation at proposed downstream TSS as proposed for Pxr[e2] (middle). In the Pxr[e2] model (middle) the DNA-binding domain remains mostly intact, though greater than half of leading zinc finger (zf1) has been deleted.

making normally rare events (ie, nonsense mutations in coding exons) more common and therefore tractable for robust scientific interrogation (Anderson *et al.*, 2017). These results may be an example of "translational plasticity" (Ma *et al.*, 2019).

An alternative explanation for retaining the wildtype response to PN exposure in the mutant animals could be the presence of an alternative pathway for sensing PN and activating the downstream transcriptional response. However, there is no precedence for this scenario, and unlike mammals, teleost fish genomes do not carry a gene for the closely related nuclear xenobiotic receptor, constitutive androstane receptor (CAR; *NR1I3*). Constitutive androstane receptor has been shown to activate *CYP3A* expression and exhibit overlap in ligand sensitivity with PXR (Timsit and Negishi, 2007; Wei *et al.*,

2002; Zhao *et al.*, 2015). The absence of CAR in teleost fish magnifies the potential importance of PXR for xenobiotic-sensing and response (Ekins *et al.*, 2008). The most closely related sequences in fish genomes (in the absence of CAR; *NR1I3*) are the vitamin D receptors (VDRa and VDRb; NR1I1a and NR1I1b). Although these have been thought to possibly substitute for the genomic lack of PXR in cod, experimental results have not supported a strong role for VDR in transcriptional responses to known PXR agonists in fish (Goksyør, personal communication). Although we cannot rule out the possibility that another nuclear receptor shares ligand specificity and transcriptional activation with *pxr*, and can compensate for its loss, the morpholino effect suggests this is not the case (Kubota *et al.*, 2015).

Despite all the transcriptional evidence, this study lacks direct evidence for truncated protein translated from the mutant mRNA. We and others have not been able to successfully use commercially available antibodies putatively specific for zebrafish Pxr, nor have efforts to produce a monoclonal antibody been successful (Goksyør, personal communication). To this end, we have efforts underway to generate zebrafish with their endogenous *pxr* locus modified to include a C-terminal epitope tag on the coding region. N-terminal epitope tags appear to inhibit *pxr* translation (data not shown). Progress on this front will enable visualization of endogenous Pxr localization, and enable chromatin immunoprecipitation and protein-protein interaction assays, which will provide more direct evidence for the role of Pxr in the zebrafish chemical defensome.

CONCLUSION

In conclusion, our data suggest a compensatory mechanism is responsible for the PN response in zebrafish *pxr* mutants. Two alternative possibilities might also explain the outcomes: either Pxr is not required for PN-induced expression of *cyp3a65*, or a severely truncated mutant Pxr is responsible for the pregnenolone response. We are actively carrying out follow-up experiments to address these uncertainties including the generation of 2 more *pxr* CRISPR mutants, 1 targeting exon 3 and the other exon 6 that should effectively remove the majority of the DBD or LBD, respectively, and transactivation assays for mutant zebrafish Pxr using human PXR response elements.

DECLARATION OF CONFLICTING INTERESTS

The author/authors declared no potential conflicts of interest with respect to the research, authorship, and/or publication of this article.

SUPPLEMENTARY DATA

Supplementary data are available at *Toxicological Sciences* online.

REFERENCES

Anderson, J. L., Mulligan, T. S., Shen, M. C., Wang, H., Scahill, C. M., Tan, F. J., Du, S. J., Busch-Nentwich, E. M., and Farber, S. A. (2017). mRNA processing in mutant zebrafish lines generated by chemical and CRISPR-mediated mutagenesis produces unexpected transcripts that escape nonsense-mediated decay. *PLoS Genet.* **13**, e1007105–18.

Azuma, K., Casey, S. C., Ito, M., Urano, T., Horie, K., Ouchi, Y., Kirchner, S., Blumberg, B., and Inoue, S. (2010). Pregnane X receptor knockout mice display osteopenia with reduced bone formation and enhanced bone resorption. *J. Endocrinol.* **207**, 257–263.

Azuma, K., Shiba, S., Hasegawa, T., Ikeda, K., Urano, T., Horie-Inoue, K., Ouchi, Y., Amizuka, N., and Inoue, S. (2015). Osteoblast-specific *γ*-glutamyl carboxylase-deficient mice display enhanced bone formation with aberrant mineralization. *J. Bone Miner. Res.* **30**, 1245–1254.

Bassett, A. R., Tibbit, C., Ponting, C. P., and Liu, J. L. (2013). Highly efficient targeted mutagenesis of *Drosophila* with the CRISPR/Cas9 system. *Cell Rep.* **4**, 220–228.

Blumberg, B., Sabbagh, W., Jr, Juguilon, H., Bolado, J., Jr, van Meter, C. M., Ong, E. S., and Evans, R. M. (1998). SXR, a novel steroid and xenobiotic sensing nuclear receptor. *Genes Dev.* **12**, 3195–3205.

Delfosse, V., Dendele, B., Huet, T., Grimaldi, M., Boulahtouf, A., Gerbal-Chaloin, S., Beucher, B., Roecklin, D., Muller, C., Rahmani, R., *et al.* (2015). Synergistic activation of human pregnane X receptor by binary cocktails of pharmaceutical and environmental compounds. *Nat. Commun.* **6**, 8089.

Dussault, I., and Forman, B. M. (2002). The nuclear receptor PXR: A master regulator of "homeland" defense. *Crit. Rev. Eukaryot. Gene Expr.* **12**, 53–64.

Eide, M., Rydbeck, H., Tørresen, O. K., Lille-Langøy, R., Puntervoll, P., Goldstone, J. V., Jakobsen, K. S., Stegeman, J., Goksøyr, A., and Karlsen, O. A. (2018). Independent losses of a xenobiotic receptor across teleost evolution. *Sci. Rep.* **8**, 1–13.

Ekins, S., Reschly, E. J., Hagey, L. R., and Krasowski, M. D. (2008). Evolution of pharmacologic specificity in the pregnane X receptor. *BMC Evol. Biol.* **8**, 103.

Fonseca, E. S. S., Ruivo, R., Machado, A. M., Conrado, F., Tay, B. H., Venkatesh, B., Santos, M. M., and Castro, L. F. C. (2019). Evolutionary plasticity in detoxification gene modules: The preservation and loss of the pregnane X receptor in chondrichthyes lineages. *Int. J. Mol. Sci.* **20**, 1–11.

Frye, C. A., Koonce, C. J., and Walf, A. A. (2014). Novel receptor targets for production and action of allopregnanolone in the central nervous system: A focus on pregnane xenobiotic receptor. *Front. Cell. Neurosci.* **8**, 1–13.

Gagnon, J. A., Valen, E., Thyme, S. B., Huang, P., Ahkmetova, L., Pauli, A., Montague, T. G., Zimmerman, S., Richter, C., and Schier, A. F. (2014). Efficient mutagenesis by Cas9 protein-mediated oligonucleotide insertion and large-scale assessment of single-guide RNAs. *PLoS One* **9**, e98186–12.

Goldstone, J. V., Hamdoun, A., Cole, B. J., Howard-Ashby, M., Nebert, D. W., Scally, M., Dean, M., Epel, D., Hahn, M. E., and Stegeman, J. J. (2006). The chemical defensome: Environmental sensing and response genes in the *Strongylocentrotus purpuratus* genome. *Dev. Biol.* **300**, 366–384.

Gräns, J., Wassmur, B., Fernández-Santoscoy, M., Zanette, J., Woodin, B. R., Karchner, S. I., Nacci, D. E., Champlin, D., Jayaraman, S., Hahn, M. E., *et al.* (2015). Regulation of pregnane-X-receptor, CYP3A and P-glycoprotein genes in the PCB-resistant killifish (*Fundulus heteroclitus*) population from New Bedford Harbor. *Aquat. Toxicol.* **159**, 198–207.

Guo, X., Zhang, T., Hu, Z., Zhang, Y., Shi, Z., Wang, Q., Cui, Y., Wang, F., Zhao, H., and Chen, Y. (2014). Efficient RNA/Cas9-mediated genome editing in *Xenopus tropicalis*. *Development* **141**, 707–714.

Hecker, N., Sharma, V., and Hiller, M. (2019). Convergent gene losses illuminate metabolic and physiological changes in herbivores and carnivores. *Proc. Natl. Acad. Sci. U.S.A.* **116**, 3036–3041.

Howe, K., Clark, M. D., Torroja, C. F., Torrance, J., Berthelot, C., Muffato, M., Collins, J. E., Humphray, S., McLaren, K., Matthews, L., *et al.* (2013). The zebrafish reference genome

sequence and its relationship to the human genome. *Nature* **496**, 498–503.

Igarashi, K., Kitajima, S., Aisaki, K., Tanemura, K., Taquahashi, Y., Moriyama, N., Ikeno, E., Matsuda, N., Saga, Y., Blumberg, B., *et al.* (2012). Development of humanized steroid and xenobiotic receptor mouse by homologous knock-in of the human steroid and xenobiotic receptor ligand binding domain sequence. *J. Toxicol. Sci.* **37**, 373–380.

Ihunnah, C. A., Jiang, M., and Xie, W. (2011). Nuclear receptor PXR, transcriptional circuits and metabolic relevance. *Biochim. Biophys. Acta* **1812**, 956–963.

Kliewer, S. A., Goodwin, B., and Willson, T. M. (2002). The nuclear pregnane X receptor: A key regulator of xenobiotic metabolism. *Endocr. Rev.* **23**, 687–702.

Kliewer, S. A., Moore, J. T., Wade, L., Staudinger, J. L., Watson, M. A., Jones, S. A., McKee, D. D., Oliver, B. B., Willson, T. M., Zetterström, R. H., *et al.* (1998). An orphan nuclear receptor activated by pregnanes defines a novel steroid signaling pathway. *Cell* **92**, 73–82.

Konno, Y., Moore, R., Kamiya, N., and Negishi, M. (2010). Nuclear xenobiotic receptor PXR-null mouse exhibits hypophosphatemia and represses the Na/Pi-cotransporter SLC34A2. *Pharmacogenet. Genomics* **20**, 9–17.

Koyano, S., Kurose, K., Saito, Y., Ozawa, S., Hasegawa, R., Komamura, K., Ueno, K., Kamakura, S., Kitakaze, M., Nakajima, T., *et al.* (2004). Functional characterization of four naturally occurring variants of human pregnane X receptor (PXR): One variant causes dramatic loss of both DNA binding activity and the transactivation of the CYP3A4 promoter/enhancer region. *Drug Metab. Dispos.* **32**, 149–154.

Krasowski, M. D., Yasuda, K., Hagey, L. R., and Schuetz, E. G. (2005). Evolution of the pregnane X receptor: Adaptation to cross-species differences in biliary bile salts. *Mol. Endocrinol.* **19**, 1720–1739.

Kubota, A., Goldstone, J. V., Lemaire, B., Takata, M., Woodin, B. R., and Stegeman, J. J. (2015). Role of pregnane X receptor and aryl hydrocarbon receptor in transcriptional regulation of pxr, CYP2, and CYP3 genes in developing zebrafish. *Toxicol. Sci.* **143**, 398–407.

Lamba, J., Lamba, V., and Schuetz, E. (2005). Genetic variants of PXR (NR1I2) and CAR (NR1I3) and their implications in drug metabolism and pharmacogenetics. *Curr. Drug Metab.* **6**, 369–383.

Lamba, V., Yasuda, K., Lamba, J. K., Assem, M., Davila, J., Strom, S., and Schuetz, E. G. (2004). PXR (NR1I2): Splice variants in human tissues, including brain, and identification of neurosteroids and nicotine as PXR activators. *Toxicol. Appl. Pharmacol.* **199**, 251–265.

Lehmann, J. M., McKee, D. D., Watson, M. A., Willson, T. M., Moore, J. T., and Kliewer, S. A. (1998). The human orphan nuclear receptor PXR is activated by compounds that regulate CYP3A4 gene expression and cause drug interactions. *J. Clin. Invest.* **102**, 1016–1023.

Lille-Langøy, R., Goldstone, J. V., Rusten, M., Milnes, M. R., Male, R., Stegeman, J. J., Blumberg, B., and Goksøyr, A. (2015). Environmental contaminants activate human and polar bear (*Ursus maritimus*) pregnane X receptors (PXR, NR1I2) differently. *Toxicol. Appl. Pharmacol.* **284**, 54–64.

Lille-Langøy, R., Karlsen, O. A., Myklebust, L. M., Goldstone, J. V., Mork-Jansson, A., Male, R., Blumberg, B., Stegeman, J. J., and Goksøyr, A. (2019). Sequence variations in pxr (NR1I2) from zebrafish (*Danio rerio*) strains affect nuclear receptor function. *Toxicol. Sci.* **168**, 28–39.

Lin, Y. S., Yasuda, K., Assem, M., Cline, C., Barber, J., Li, C. W., Kholodovych, V., Ai, N., Chen, J. D., Welsh, W. J., *et al.* (2009). The major human pregnane X receptor (PXR) splice variant, PXR.2, exhibits significantly diminished ligand-activated transcriptional regulation. *Drug Metab. Dispos.* **37**, 1295–1304.

Ma, Z., Zhu, P., Shi, H., Guo, L., Zhang, Q., Chen, Y., Chen, S., Zhang, Z., Peng, J., and Chen, J. (2019). PTC-bearing mRNA elicits a genetic compensation response via Upf3a and COMPASS components. *Nature* **568**, 259–263.

Matic, M., Corradin, A. P., Tsoli, M., Clarke, S. J., Polly, P., and Robertson, G. R. (2010). The alternatively spliced murine pregnane X receptor isoform, mPXR(delta171-211) exhibits a repressive action. *Int. J. Biochem. Cell Biol.* **42**, 672–682.

Montague, T. G., Cruz, J. M., Gagnon, J. A., Church, G. M., and Valen, E. (2014). CHOPCHOP: A CRISPR/Cas9 and TALEN web tool for genome editing. *Nucleic Acids Res.* **42**, 401–407.

Moore, L. B., Maglich, J. M., McKee, D. D., Wisely, B., Willson, T. M., Kliewer, S. A., Lambert, M. H., and Moore, J. T. (2002). Pregnane X receptor (PXR), constitutive androstane receptor (CAR), and benzoate X receptor (BXR) define three pharmacologically distinct classes of nuclear receptors. *Mol. Endocrinol.* **16**, 977–986.

Myers, C. T., and Krieg, P. A. (2013). BMP-mediated specification of the erythroid lineage suppresses endothelial development in blood island precursors. *Blood* **122**, 3929–3939.

Nakayama, T., Blitz, I. L., Fish, M. B., Odeleye, A. O., Manohar, S., Cho, K. W. Y., and Grainger, R. M. (2014). Cas9-based Genome Editing in Xenopus Tropicalis. *Genesis*, **51**, 835–884.

Spruiell, K., Gyamfi, A. A., Yeyeodu, S. T., Richardson, R. M., Gonzalez, F. J., and Gyamfi, M. A. (2015). Pregnane X Receptor-humanized mice recapitulate gender differences in ethanol metabolism but not hepatotoxicity. *J. Pharmacol. Exp. Ther.* **354**, 459–470.

Stegeman, J. J., Goldstone, J. V., and Hahn, M. E. (2010). Perspectives on Zebrafish as a Model in Environmental Toxicology. *Fish Physiology.* **29**, 367–439.

Timsit, Y. E., and Negishi, M. (2007). CAR and PXR: The xenobiotic-sensing receptors. *Steroids* **72**, 231–246.

Tirona, R. G., Leake, B. F., Podust, L. M., and Kim, R. B. (2004). Identification of amino acids in rat pregnane X receptor that determine species-specific activation. *Mol. Pharmacol.* **65**, 36–44.

Wei, P., Zhang, J., Dowhan, D. H., Han, Y., and Moore, D. D. (2002). Specific and overlapping functions of the nuclear hormone receptors CAR and PXR in xenobiotic response. *Pharmacogenomics J.* **2**, 117–126.

Westerfield, M. (2000). *The Zebrafish Book. A Guide for the Laboratory Use of Zebrafish (Danio rerio)*. University of Oregon Press, Eugene.

Xie, W., Barwick, J. L., Downes, M., Blumberg, B., Simon, C. M., Nelson, M. C., Neuschwander-Tetri, B. A., Brunt, E. M., Guzelian, P. S., and Evans, R. M. (2000). Humanized xenobiotic response in mice expressing nuclear receptor SXR. *Nature* **406**, 435–439.

Yates, A., Akanni, W., Amode, M. R., Barrell, D., Billis, K., Carvalho-Silva, D., Cummins, C., Clapham, P., Fitzgerald, S., Gil, L., *et al.* (2016). Ensembl 2016. *Nucleic Acids Res.* **44**, D710–716.

Zhao, Y., Zhang, K., Giesy, J. P., and Hu, J. (2015). Families of nuclear receptors in vertebrate models: Characteristic and comparative toxicological perspective. *Sci. Rep.* **5**, 8554.

Zhou, C., Verma, S., and Blumberg, B. (2009). The steroid and xenobiotic receptor (SXR), beyond xenobiotic metabolism. *Nucl. Recept. Signal.* **7**, e001.